



OPEN ACCESS

EDITED BY

Guangming Xu,
Beijing Normal University, Zhuhai, China

REVIEWED BY

Jessica Arnall,
University of Edinburgh, United Kingdom
Xiang Zhang,
Hainan University, China

*CORRESPONDENCE

Shaochun Xu
✉ xushaochun@qdio.ac.cn
Yi Zhou
✉ yizhou@qdio.ac.cn

RECEIVED 03 December 2025

REVISED 20 January 2026

ACCEPTED 26 January 2026

PUBLISHED 12 February 2026

CITATION

Xu S, Yin G, Wang X, Yuan Y, Wang Y, Liu M, Zhang Y, Yue S, Zhang X and Zhou Y (2026) Light outweighs ammonium: irradiance governs early morphological, physiological and isotopic responses of *Zostera marina* under controlled nutrient additions. *Front. Mar. Sci.* 13:1752748. doi: 10.3389/fmars.2026.1752748

COPYRIGHT

© 2026 Xu, Yin, Wang, Yuan, Wang, Liu, Zhang, Yue, Zhang and Zhou. This is an open-access article distributed under the terms of the [Creative Commons Attribution License \(CC BY\)](https://creativecommons.org/licenses/by/4.0/). The use, distribution or reproduction in other forums is permitted, provided the original author(s) and the copyright owner(s) are credited and that the original publication in this journal is cited, in accordance with accepted academic practice. No use, distribution or reproduction is permitted which does not comply with these terms.

Light outweighs ammonium: irradiance governs early morphological, physiological and isotopic responses of *Zostera marina* under controlled nutrient additions

Shaochun Xu^{1,2,3,4*}, Guangwei Yin⁵, Xinhua Wang^{1,4}, Yuan Yuan⁵, Yibo Wang^{1,4}, Mingjie Liu^{1,4}, Yu Zhang^{1,2,3}, Shidong Yue^{1,2,3}, Xiaomei Zhang^{1,2,3} and Yi Zhou^{1,2,3,4*}

¹Laboratory of Marine Ecology and Environmental Sciences, Institute of Oceanology, Chinese Academy of Sciences, Qingdao, China, ²Laboratory for Marine Ecology and Environmental Science, Qingdao Marine Science and Technology Center, Qingdao, China, ³Field Scientific Observation and Research Station of Yellow-Bohai Sea Temperate Seagrass Bed Ecosystems, Ministry of Natural Resources, Qingdao, China, ⁴University of Chinese Academy of Sciences, Beijing, China, ⁵College of Environment and Safety Engineering, Qingdao University of Science and Technology, Qingdao, China

Under accelerating coastal eutrophication, disentangling the relative roles of light limitation and nitrogen enrichment is essential for diagnosing seagrass decline. We conducted a fully crossed light × ammonium experiment using intact *Zostera marina* cores from Guzhenkou Bay (4 irradiance levels: 180, 90.6, 17, 0 μmol photons m⁻² s⁻¹; 4 NH₄Cl levels: 0, 25, 50, 100 μmol L⁻¹; 5 weeks; 16 units; no within-cell replication). Across traits, irradiance—not NH₄Cl within the tested range—governed responses at the level of dominant main effects. Shading sharply reduced shoot density, above- and below-ground biomass (AGB, BGB) and F_v/F_m, with near-complete collapse at darkness. Biomass turnover accelerated under shading (higher above-ground shedding, below-ground mass loss), and below-ground carbon content declined, together indicating a shift from carbon accrual to expenditure. By contrast, NH₄Cl enrichment showed minimal main effects on morphology, pigments, F_v/F_m, or antioxidant enzymes, although tissue δ¹⁵N decreased with NH₄Cl addition, evidencing ammonium assimilation. Antioxidant responses were variable (POD increased with reduced irradiance; SOD, CAT, GSH-Px inconsistent), while MDA did not increase under shading and was occasionally higher under high light, consistent with lower photo-oxidative load at low irradiance. Leaf and rhizome δ¹³C showed no significant treatment effects and only a weak, non-significant tendency toward less negative values under severe shading. Collectively, the trait suite diagnoses light-driven carbon limitation as the proximal stressor, with nitrogen

effects contingent on concentration and context. We recommend tiered monitoring that couples rapid photophysiology (F_v/F_m) with structural (shoot density, AGB/BGB) and integrative biogeochemical indicators (below-ground C; δ -isotopes), and management focused on water clarity to meet species-specific light requirements.

KEYWORDS

ammonium enrichment, antioxidant defense, light limitation, photosynthesis, *Zostera marina* L., δ -isotopes

1 Introduction

Seagrass meadows provide foundational coastal services—stabilizing sediments, sequestering carbon, and supporting fisheries (Unsworth et al., 2018; Kent et al., 2021; Serrano et al., 2021). Yet many populations persist close to their light limits, making them highly sensitive to turbidity pulses and chronic eutrophication (Ralph et al., 2007; Bulmer et al., 2018; Van Katwijk et al., 2024). Although nutrient supply can alter growth and physiology, restoration trajectories often hinge on maintaining a positive carbon balance, which is primarily governed by irradiance at the canopy (Ralph et al., 2007). Accordingly, disentangling the roles of light and nitrogen remains both a practical and theoretical priority for management and recovery planning (Ralph et al., 2007; Van Katwijk et al., 2024).

Zostera marina is a foundation species widely distributed in temperate coastal ecosystems of the Northern Hemisphere (Green and Short, 2003; Olsen et al., 2016). Importantly, *Z. marina* has been extensively used as a model seagrass species in studies examining light limitation (Bertelli and Unsworth, 2018) and nutrient enrichment (Van Katwijk et al., 1997), providing a well-established empirical basis for evaluating how irradiance and ammonium availability jointly shape early growth trajectories under controlled conditions relevant to coastal eutrophication.

Light governs both instantaneous photochemistry and whole-plant carbon economics in seagrasses: when irradiance drops below compensation, positive carbon balance cannot be maintained, precipitating growth decline and range contraction (Ralph et al., 2007). Consistent with this framework, short-term shading rapidly depletes rhizome and root non-structural carbohydrates (NSC) and reduces biomass and shoot density, reflecting a shift from carbon accrual to carbon expenditure (Burke et al., 1996; Wong et al., 2021). Early-warning signals of this transition typically include declines in photophysiology (F_v/F_m), suppressed leaf extension, and reductions in above- and below-ground biomass, often accompanied by accelerated tissue turnover (senescent leaf loss and below-ground mass loss) (Burke et al., 1996; Ralph et al., 2007; Wong et al., 2021). At the same time, as excitation pressure wanes, chloroplast redox control follows a ‘push–pull’ behavior in which reactive oxygen species (ROS) generation depends on light-driven reductant supply, so oxidative damage does not necessarily intensify under shading (Foyer and Noctor, 2016).

Nitrogen supply can modulate the light-driven trajectory in two opposing ways. Low–moderate enrichment may alleviate nutrient limitation and transiently stimulate growth, whereas high ammonium (NH_4^+) or co-stress with low light imposes metabolic

costs and can become toxic (Van Katwijk et al., 1997; Touchette and Burkholder, 2000). Mechanistically, low irradiance enhances ammonium toxicity because photosynthesis and the carbon stores required to assimilate NH_4^+ into amino acids are reduced (Collos and Harrison, 2014), consistent with reports that elevated ammonium and low light form a dangerous synergy for eelgrass (Villazán et al., 2013). Importantly, the magnitude and direction of nitrogen effects depend strongly on dose, exposure duration, and light context, highlighting the need to evaluate nitrogen responses within ecologically realistic concentration ranges rather than assuming uniformly negative effects (Van Katwijk et al., 1997; Touchette and Burkholder, 2000). Critically, nitrogen effects depend on dose, exposure duration and light context; therefore, diagnosing limitation is best achieved with a multi-metric suite spanning morphology (shoot density/biomass), photophysiology (F_v/F_m) and, where feasible, biogeochemistry (NSC, δ -isotopes) rather than reliance on a single indicator (McMahon et al., 2013; Collier et al., 2016; Roca et al., 2016; Statton et al., 2017). Within this framework, antioxidant enzyme activities (e.g. SOD, CAT, GSH-Px, POD) and lipid peroxidation products (MDA) provide complementary indicators of cellular redox balance and photo-oxidative stress, allowing discrimination between carbon limitation driven by light reduction and stress responses associated with excess excitation energy (Foyer and Noctor, 2016; Bertelli and Unsworth, 2018).

Here, we employed intact *Z. marina* cores from Guzhengkou Bay in a fully crossed 4×4 irradiance (180, 90.6, 17, 0 $\mu\text{mol photons m}^{-2} \text{s}^{-1}$) \times NH_4Cl addition (0, 25, 50, 100 $\mu\text{mol L}^{-1}$) matrix over five weeks. The experimental gradients were designed to represent generalized light and ammonium conditions relevant to coastal eutrophication, rather than to reproduce site-specific environmental conditions at Guzhengkou Bay. The selected ammonium concentrations span background to elevated levels commonly reported in eutrophic coastal waters, while remaining below or near thresholds previously associated with acute toxicity in *Z. marina*, thereby enabling assessment of dose-dependent responses under contrasting light regimes (Van Katwijk et al., 1997; Villazán et al., 2013). Our aim was to determine whether irradiance or ammonium enrichment exerts the dominant control on early structural, physiological and isotopic responses. We quantified (i) structural metrics (shoot density, leaf length, above- and below-ground biomass, leaf shedding rate and below-ground mass loss), (ii) photophysiological/pigment parameters (F_v/F_m , Rubisco activity, chlorophyll a and b), (iii) antioxidant enzyme activities (SOD, CAT, GSH-Px, POD) and malondialdehyde (MDA), and (iv) elemental/isotopic composition (C, N, $\delta^{13}\text{C}$, $\delta^{15}\text{N}$). Because each light \times nutrient cell lacked replicates, we restricted inference to

main effects of irradiance and ammonium, acknowledging that interaction effects are confounded with residual error. We hypothesized that (1) irradiance would dominate responses across hierarchical levels—indicative of carbon limitation under shading, (2) within the tested ammonium range, NH_4Cl alone would induce minimal structural or photophysiological effects but would be traceable isotopically via declining $\delta^{15}\text{N}$, and (3) antioxidant enzyme and MDA responses would reflect reduced photo-oxidative load under low irradiance rather than increased oxidative damage. Our results support these hypotheses and suggest a tiered, field-transferable monitoring framework aligning rapid photophysiology with structural and isotopic indicators, while reaffirming water-clarity (and thus canopy irradiance) as the primary management focus.

2 Materials and methods

2.1 Sampling and experimental design

A total of sixteen undisturbed seagrass–sediment cores were collected from Guzhenkou Bay. Sampling was conducted using PVC cylinders (18 cm outer diameter, 17.69 cm inner diameter, 15 cm height). After being carefully excavated with a shovel, each core was sealed in a zip-lock bag and secured within the PVC cylinder using adhesive tape to preserve its natural structure. All cores were then placed in insulated containers with ice packs and immediately transported to the laboratory. After collection and transport (Day 1), cores were allowed to recover overnight under controlled laboratory conditions. On Day 2, experimental treatments were initiated immediately thereafter, without an extended acclimation period.

In the laboratory, each core was standardized to three shoots trimmed to 30 cm in height and transferred to an individual aerated seawater pot (inner diameter 19.5 cm, height 80 cm; $23 \pm 1^\circ\text{C}$; 12 h light: 12 h dark). To minimize variation in initial plant size and biomass among experimental units, all cores were visually inspected prior to treatment initiation, and only intact cores with comparable shoot vigor, morphology, and sediment structure were selected. The number of shoots per core was fixed ($n = 3$), reflecting typical shoot densities observed in the source meadow and allowing sufficient biomass for subsequent analyses while minimizing within-core self-shading. Shoot height was standardized to 30 cm to ensure comparable initial aboveground biomass and canopy structure across treatments. Initial leaf number per shoot was not explicitly quantified; however, the above visual selection ensured comparable leaf development and overall plant condition among experimental units.

A fully crossed 4×4 irradiance \times nutrient matrix was established, with one experimental unit per treatment combination (i.e., no within-treatment replication). Irradiance was set to 180 (high light; H), 90.6 (medium light; M), 17 (low light; L) or 0 (darkness; EL) $\mu\text{mol photons m}^{-2} \text{s}^{-1}$ using dimmable LED arrays fitted with neutral-density shade screens or blackout cloth; four NH_4Cl addition levels were applied, corresponding to

(control; CK), 25 (low N addition; L), 50 (medium N addition; M), and 100 (high N addition; H) $\mu\text{mol L}^{-1}$ added relative to background concentrations. Seawater was renewed weekly, and following each renewal NH_4Cl was re-added to re-establish the target concentrations for each treatment (Figure 1).

Sixteen intact seagrass–sediment cores (one per treatment combination; no within-treatment replication) were exposed to four PPFD levels (180, 90.6, 17, and 0 $\mu\text{mol m}^{-2} \text{s}^{-1}$) using dimmable LED panels with neutral-density shade screens or blackout cloth, and four NH_4Cl addition levels (added concentrations of 0, 25, 50, and 100 $\mu\text{mol L}^{-1}$). Cores were maintained in aerated seawater pots under controlled temperature and photoperiod conditions. The schematic diagram was generated from an AI-produced illustration (ChatGPT 5.2) and subsequently refined to accurately represent the experimental design.

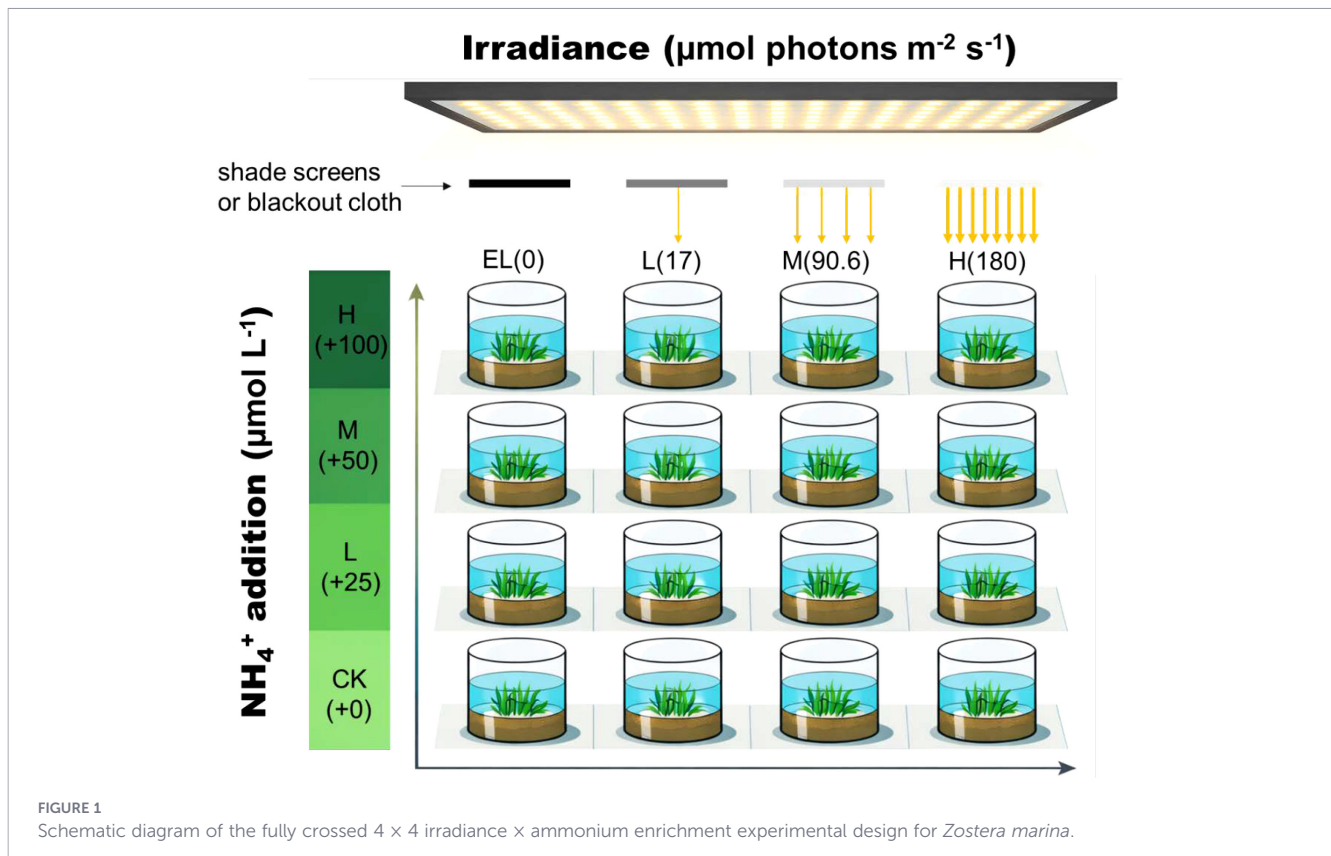
Because intact seagrass–sediment cores were used as experimental units, belowground biomass and sediment conditions were preserved at collection. Although initial belowground biomass could not be destructively quantified prior to treatment, the use of undisturbed cores from the same meadow and the above standardization procedures were intended to minimize among-treatment variability at the start of the experiment. Consequently, post-treatment differences in morphological traits are attributed primarily to experimental treatments rather than to initial heterogeneity among cores.

The experimental duration was set to five weeks to capture early-stage physiological and morphological responses of *Z. marina* to changes in irradiance and ammonium availability. During preliminary observations and the course of the experiment, seagrass growth remained relatively stable across most treatments during the first four weeks. However, pronounced shoot mortality began to occur during the fifth week, particularly under low-irradiance conditions. The experiment was therefore terminated at five weeks to avoid confounding early treatment responses with severe light-induced mortality, which would have precluded reliable measurement of early physiological and morphological changes.

At the end of the experiment, samples were harvested for subsequent analyses. Photosynthetic parameters were determined to evaluate seagrass photosynthetic performance. Additional samples were collected for measurements of morphological attributes, enzymatic activities, carbon and nitrogen concentrations, and the stable isotopic composition of these elements. In a limited number of treatments, biomass loss toward the end of the experiment restricted the measurement of certain variables due to insufficient remaining material.

2.2 Morphological analysis

Upon completion of the experiment, shoots per pot were counted, and leaf lengths were measured. Above- and belowground tissues were carefully separated, oven-dried at 60°C until constant mass, and weighed. Fallen leaves and dead belowground tissue fragments were collected at the end of the experiment, dried, and weighed. The aboveground shedding rate (AGR) was calculated as the proportion of fallen leaf biomass



relative to the sum of fallen leaves and standing live aboveground biomass. Similarly, the belowground decomposition rate (BGR) was calculated as the proportion of dead belowground tissue fragments relative to the sum of dead and live belowground biomass. These metrics represent end-point proportional indicators of tissue turnover rather than continuous time-based rates.

2.3 Physiological analysis

The maximum quantum yield of PSII (Fv/Fm) in eelgrass leaves was measured using a Diving-PAM fluorometer (Walz, Germany). Prior to measurement, plants were dark-adapted for 30 min to ensure full relaxation of PSII reaction centers. Measurements were taken 2–5 cm above the sheath of the second youngest leaf, following the protocol of Zhang et al. (2024). One measurement was conducted per treatment. Leaf blades were collected from each treatment. Chlorophyll a (Chl a) and chlorophyll b (Chl b) contents were quantified according to Lichtenthaler (1987). To evaluate photosynthetic carbon fixation capacity, Rubisco activity was assessed following Makino et al. (1985) with minor modifications. Enzymatic antioxidant defenses and redox regulation under contrasting light and ammonium conditions were evaluated by determining the activities of superoxide dismutase (SOD), catalase (CAT), glutathione peroxidase (GSH-Px), and peroxidase (POD) according to Dazy et al. (2009). Lipid peroxidation was evaluated by measuring malondialdehyde (MDA) content following the method of Hodges et al. (1999), providing an index of oxidative membrane damage. Together, these biochemical assays were used to diagnose oxidative stress status and cellular damage associated with

combined light and nutrient treatments. All biochemical analyses were performed by Wilmin Biotechnology (Suzhou, China).

2.4 Elemental/isotope analysis

Dried tissues were finely homogenized and sieved prior to elemental and isotope analyses. Carbon and nitrogen concentrations were determined with a Vario EL III CHNS elemental analyzer (Elementar Analysensysteme GmbH,

TABLE 1 Analysis of variance results for the effects of light intensity and NH_4Cl enrichment on morphological parameters.

Parameter	Source of variation	F	P	partial η^2
Shoot density	Irradiance	18.23	< 0.001	0.9
	NH_4Cl	1.62	0.253	0.45
Leaf length	Irradiance	3.25	0.102	0.62
	NH_4Cl	1.48	0.312	0.43
Aboveground biomass	Irradiance	8.7	0.013	0.81
	NH_4Cl	0.99	0.457	0.33
Belowground biomass	Irradiance	9.75	0.005	0.83
	NH_4Cl	0.73	0.56	0.27
Aboveground shedding rate	Irradiance	13.31	0.001	0.87
	NH_4Cl	1.03	0.426	0.34
Belowground decomposition rate	Irradiance	7.94	0.007	0.8
	NH_4Cl	3.38	0.068	0.63

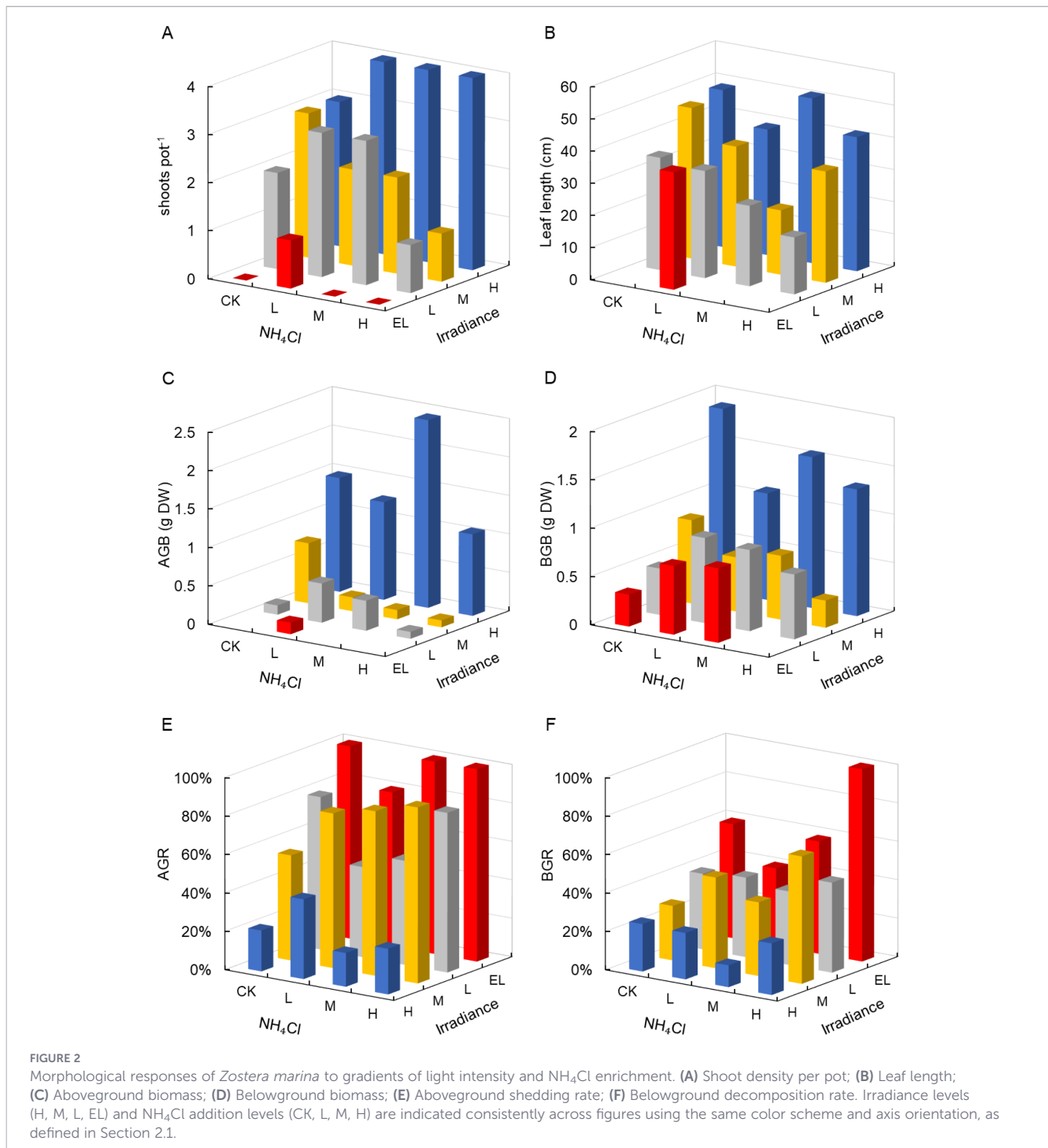
Germany) and expressed on a dry-weight basis; C:N ratios are reported on a molar scale. Stable isotope compositions ($\delta^{13}\text{C}$ and $\delta^{15}\text{N}$) were analyzed using a Flash EA 1112 elemental analyzer coupled to a Delta V Advantage isotope ratio mass spectrometer (Thermo Fisher Scientific, USA). Isotopic values are expressed in delta (δ) notation:

$$\delta(\text{‰}) = [(R_{\text{sample}}/R_{\text{standard}}) - 1] \times 1000$$

relative to Vienna Pee Dee Belemnite (V-PDB) for carbon and atmospheric N_2 for nitrogen. Analytical precision (± 1 SD) was $\pm 0.08 \text{ ‰}$ for $\delta^{13}\text{C}$ and $\pm 0.20 \text{ ‰}$ for $\delta^{15}\text{N}$, based on replicate analyses.

2.5 Data analyses

Prior to hypothesis testing, data were tested for normality using the one-sample Kolmogorov–Smirnov test. Variables that deviated from normality (aboveground shedding rate, MDA, and belowground $\delta^{15}\text{N}$) were square-root or square transformed before analysis. These transformations were applied solely to improve adherence to model assumptions; biological interpretation focuses on the direction and relative magnitude of treatment effects rather than on transformed-scale values. Homogeneity of variances was assessed visually from residual



plots, as Levene’s test is not applicable in a 2-factor design without replication. A 2-way analysis of variance without replication was used to evaluate the main effects of irradiance and NH₄Cl addition on response variables. Accordingly, statistical inference was restricted to the main effects of irradiance and ammonium, and interaction effects were not interpreted. As statistical inference in this unreplicated factorial design is restricted to main effects, all results reported below describe main effects of irradiance and NH₄Cl enrichment and should be interpreted cautiously. When a significant main effect was detected ($p < 0.05$), *post hoc* comparisons among factor levels were used descriptively. Statistical analyses were performed using IBM SPSS Statistics 23 (IBM Corp., Armonk, NY, USA), and p -values < 0.05 were considered statistically significant.

3 Results

3.1 Morphological responses

Light intensity significantly affected most morphological traits of *Zostera marina*, while NH₄Cl enrichment alone had no significant main effects (Table 1). Shoot density differed markedly among irradiance levels ($p < 0.001$, partial $\eta^2 = 0.90$), with no shoots surviving under darkness (EL) in most treatments except EL–L (Figure 2A). This isolated survival likely reflects stochastic variation among intact cores rather than a systematic treatment effect. In contrast, plants exposed to high irradiance (H) maintained the highest shoot density (3–4 shoots pot⁻¹), followed by medium (M) and low light (L) conditions.

Leaf length showed a similar light-dependent trend, although the effect of irradiance was not statistically significant ($p = 0.102$, partial $\eta^2 = 0.62$; Table 1). Under H conditions, leaves reached 51 cm (H–M), while leaf elongation was strongly suppressed under EL (Figure 2B).

Aboveground biomass (AGB) and belowground biomass (BGB) were both significantly affected by differences among irradiance levels, indicating a graded main effect of irradiance ($p = 0.013$, partial $\eta^2 = 0.81$, and $p = 0.005$, partial $\eta^2 = 0.83$, respectively; Table 1). The highest AGB was observed under H–M (2.44 g DW pot⁻¹), while AGB declined to 0.15 g DW under EL (Figure 2C), with these treatment combinations presented as illustrative examples of the overall main effect of irradiance rather than indicative of interaction effects. BGB followed a similar pattern, peaking at 1.1–1.9 g DW under H but declining sharply under shading (Figure 2D).

Biomass turnover metrics also responded significantly to light. Aboveground shedding rate (AGR) increased under reduced irradiance ($p = 0.001$, partial $\eta^2 = 0.87$), exceeding 80–100% in EL treatments (Figure 2E). In individual cells (illustrative only), belowground decomposition rate (BGR) was highest under EL–H and M–H (up to 66–100%; $p = 0.007$, partial $\eta^2 = 0.80$; Figure 2F). NH₄Cl enrichment did not significantly affect AGR or BGR.

3.2 Physiological responses

Photosynthetic performance (Fv/Fm) was strongly affected by light ($p = 0.002$, partial $\eta^2 = 0.92$), while NH₄Cl had no significant effect (Table 2). Under H conditions, Fv/Fm remained stable at

TABLE 2 Analysis of variance results for the effects of light intensity and NH₄Cl enrichment on physiological parameters.

Parameter	Source of variation	F	P	partial η^2
Fv/Fm	Irradiance	22.76	0.002	0.92
	NH ₄ Cl	0.12	0.947	0.06
Rubisco	Irradiance	2.17	0.21	0.46
	NH ₄ Cl	1.85	0.255	0.53
chl _a	Irradiance	4.88	0.067	0.66
	NH ₄ Cl	0.8	0.543	0.32
chl _b	Irradiance	5.21	0.06	0.68
	NH ₄ Cl	0.92	0.494	0.36
chl	Irradiance	5.02	0.064	0.67
	NH ₄ Cl	0.84	0.527	0.34

0.81–0.82 across all NH₄Cl levels (Figure 3), whereas values declined markedly under M (0.56–0.69) and L (0.13–0.39) light, and were < 0.20 under EL.

Rubisco activity tended to decrease under shading but showed no significant main effects of light or NH₄Cl (Table 2; Figure 4A). The highest and lowest values occurred in specific treatment combinations (e.g., higher under H–CK/H–L and lower under L–L/L–M), but these are reported as descriptive extremes rather than statistically supported differences, given that interaction effects and within-cell contrasts are not assessed in this unreplicated design.

Chlorophyll a, chlorophyll b, and total chlorophyll content showed a descriptive tendency to decrease under shading (Figures 4B–D); however, the main effect of irradiance did not reach the $\alpha = 0.05$ threshold ($p = 0.067$, 0.060, and 0.064 for Chl a, Chl b and total Chl, respectively; partial $\eta^2 = 0.66$ –0.68), and NH₄Cl remained non-significant (Table 2). Consistent with this near-significant trend, total chlorophyll was highest under H (2.0–2.94 mg g⁻¹) and was lower under L (Figure 4D).

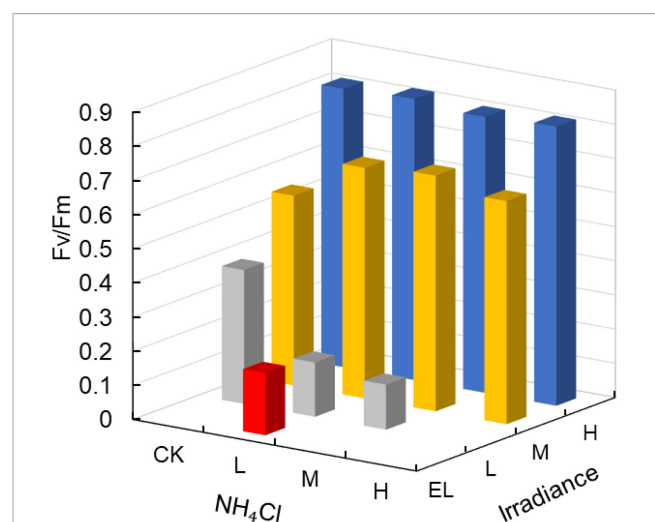


FIGURE 3 Photosynthetic performance (Fv/Fm) of *Zostera marina* under gradients of light intensity and NH₄Cl enrichment. Irradiance levels (H, M, L, EL) and NH₄Cl addition levels (CK, L, M, H) are indicated consistently across figures using the same color scheme and axis orientation, as defined in Section 2.1.

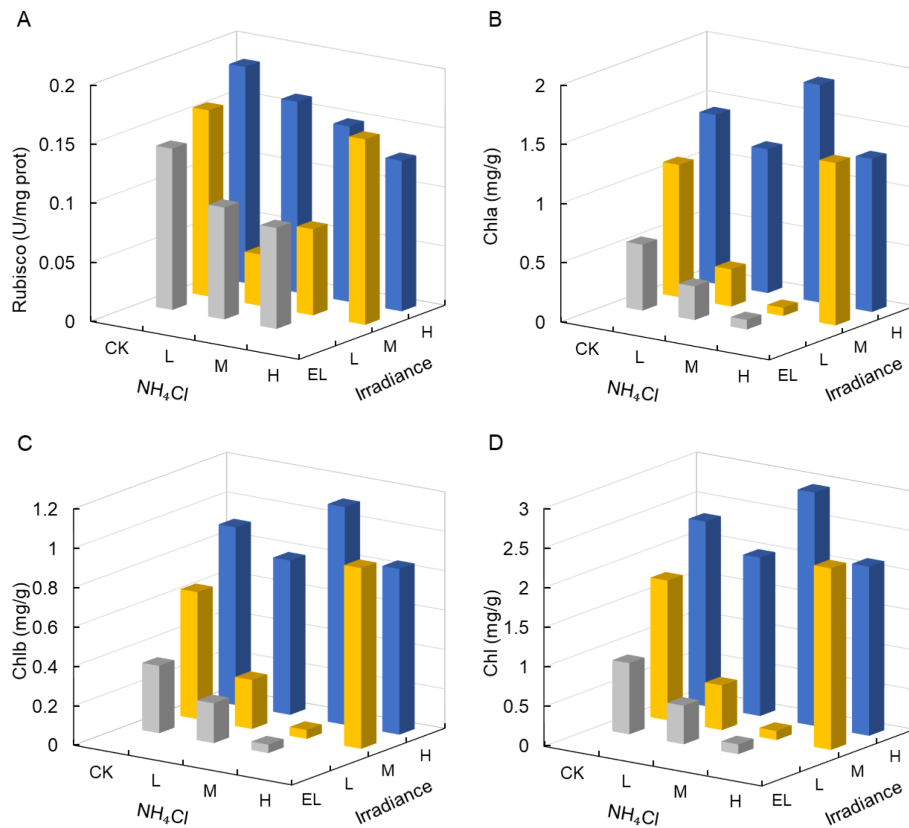


FIGURE 4 Rubisco activity and photosynthetic pigment concentrations in *Zostera marina* under gradients of light intensity and NH_4Cl enrichment. (A) Rubisco activity, (B) chlorophyll a, (C) chlorophyll b, and (D) total chlorophyll. Irradiance levels (H, M, L, EL) and NH_4Cl addition levels (CK, L, M, H) are indicated consistently across figures using the same color scheme and axis orientation, as defined in Section 2.1.

Superoxide dismutase (SOD), catalase (CAT), and glutathione peroxidase (GSH-Px) showed no significant main effects of irradiance or NH_4Cl (Table 3). However, SOD tended to be highest under L-CK (731.77 U mg^{-1} prot; Figure 5A).

In contrast, peroxidase (POD), a broad-spectrum enzyme involved in hydrogen peroxide scavenging and cell wall-associated oxidative processes, responded strongly to irradiance ($p < 0.001$, partial $\eta^2 = 0.96$; Table 3), with higher values generally observed

under reduced irradiance (Figure 5B). CAT and GSH-Px activities showed variable but non-significant trends (Figures 5C, E).

Lipid peroxidation (MDA) did not differ significantly among treatments ($p > 0.05$; Table 3). While higher MDA values were observed in some high-irradiance combinations (up to 21.56 nmol mg^{-1} prot; Figure 5D), these differences are reported descriptively and should not be interpreted as statistically supported contrasts.

3.3 Elemental/isotope responses

Carbon and nitrogen content of aboveground tissues were not significantly affected by irradiance or NH_4Cl ($p > 0.05$; Table 4), whereas belowground carbon content showed a significant response to light ($p = 0.003$, partial $\eta^2 = 0.85$; Figures 6A–D). C:N ratios remained relatively stable across treatments (Figures 6E, F).

Stable carbon isotope composition ($\delta^{13}\text{C}$) showed no significant treatment effects ($p = 0.10$ aboveground, $p = 0.22$ belowground; Table 4). Nevertheless, Figures 7A, B suggests a descriptive tendency toward less negative $\delta^{13}\text{C}$ under shading (e.g., -11.37‰ in EL-L versus -14 to -16.48‰ under high light), which is presented as an illustrative pattern rather than a statistically supported treatment effect. Accordingly, mechanistic interpretations are framed cautiously and should be considered hypothesis-generating under the constraints of the design.

Stable nitrogen isotope composition ($\delta^{15}\text{N}$) in aboveground tissues was significantly influenced by NH_4Cl enrichment ($p =$

TABLE 3 Analysis of variance results for the effects of light intensity and NH_4Cl enrichment on antioxidant enzyme activities and malondialdehyde (MDA) content.

Parameter	Source of variation	F	P	partial η^2
SOD	Irradiance	1.02	0.425	0.29
	NH_4Cl	1.95	0.24	0.54
POD	Irradiance	56.68	<0.001	0.96
	NH_4Cl	3.91	0.088	0.7
CAT	Irradiance	2.37	0.189	0.49
	NH_4Cl	0.15	0.925	0.08
MDA	Irradiance	3.58	0.109	0.59
	NH_4Cl	1.39	0.347	0.45
GSH-Px	Irradiance	0.99	0.436	0.28
	NH_4Cl	2.56	0.168	0.61

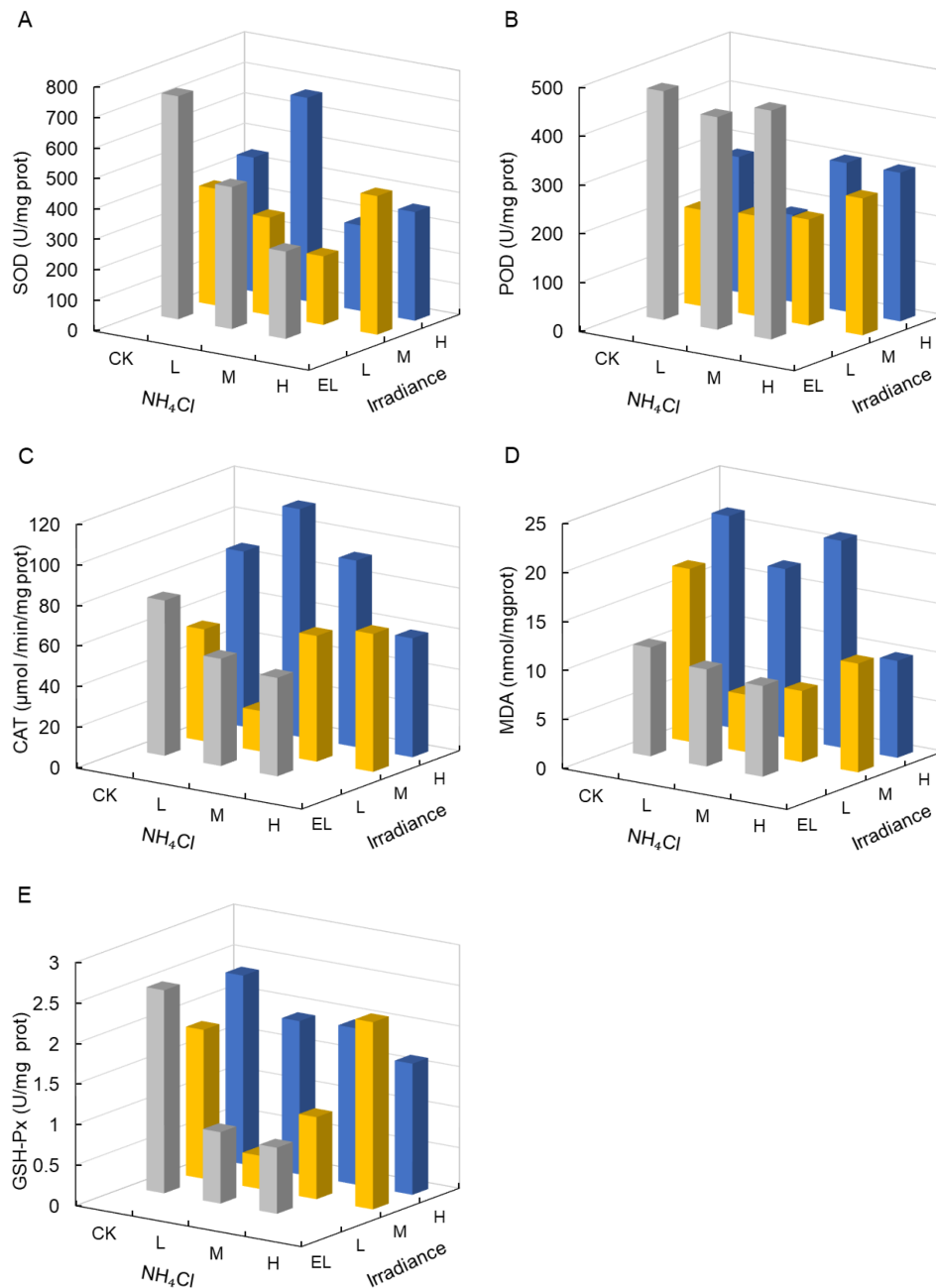


FIGURE 5 Antioxidant enzyme activities and malondialdehyde (MDA) content in *Zostera marina* under gradients of light intensity and NH_4Cl enrichment. **(A)** SOD; **(B)** POD; **(C)** CAT; **(D)** MDA; **(E)** GSH-Px. Irradiance levels (H, M, L, EL) and NH_4Cl addition levels (CK, L, M, H) are indicated consistently across figures using the same color scheme and axis orientation, as defined in Section 2.1.

0.023, partial $\eta^2 = 0.77$), with $\delta^{15}\text{N}$ decreasing from a range of 5.11–8.02‰ in the CK treatments (based on measured values) to < 4‰ under high NH_4Cl (Figure 7C). Belowground $\delta^{15}\text{N}$ also declined markedly with NH_4Cl ($p < 0.001$, partial $\eta^2 = 0.96$; Figure 7D), indicating assimilation of ^{15}N -depleted ammonium.

4 Discussion

Our results indicate that irradiance, rather than NH_4Cl enrichment within the tested range, dominated the observed early

responses of *Zostera marina* across morphological and physiological traits. Importantly, because this fully crossed design lacked within-cell replication, statistical inference is restricted to main effects only; thus, the discussion below interprets patterns as evidence of dominant main effects and does not test or attribute causality to specific light \times NH_4Cl combinations.

Pronounced declines in shoot density, AGB, BGB, and F_v/F_m under shading are consistent with the classic light-requirement theory for seagrasses, which states that most species require at least 10–20% of surface irradiance to maintain a positive carbon balance (Duarte, 1991; Dennison et al., 1993; Duarte et al., 2005; Ballesteros et al., 2007). For *Z. marina*, minimum light thresholds of

TABLE 4 Analysis of variance results for the effects of light intensity and NH₄Cl enrichment on carbon and nitrogen contents, C:N ratios, and stable isotope composition.

Tissue	Parameter	Source of variation	F	P	partial η^2
Aboveground	C	Irradiance	0.62	0.628	0.24
		NH ₄ Cl	0.7	0.586	0.26
	N	Irradiance	1.11	0.416	0.36
		NH ₄ Cl	0.04	0.987	0.02
	C/N	Irradiance	1.21	0.385	0.38
		NH ₄ Cl	0.23	0.872	0.1
	$\delta^{13}\text{C}$	Irradiance	3.25	0.102	0.62
		NH ₄ Cl	1.91	0.229	0.49
$\delta^{15}\text{N}$	Irradiance	1.2	0.386	0.38	
	NH ₄ Cl	6.88	0.023	0.78	
Belowground	C	Irradiance	11.2	0.003	0.85
		NH ₄ Cl	3.92	0.054	0.66
	N	Irradiance	0.34	0.795	0.15
		NH ₄ Cl	1.13	0.395	0.36
	C/N	Irradiance	0.44	0.732	0.18
		NH ₄ Cl	1.34	0.329	0.4
	$\delta^{13}\text{C}$	Irradiance	2.92	0.1	0.59
		NH ₄ Cl	0.55	0.66	0.22
	$\delta^{15}\text{N}$	Irradiance	1.74	0.236	0.47
NH ₄ Cl		44.79	<0.001	0.96	

approximately 10% of surface irradiance have been reported [e.g., 11% SI in a Danish embayment; (Lee et al., 2007)], below which shoot mortality and biomass loss may occur. This response is attributed to the fact that, below the compensation irradiance, respiration exceeds photosynthesis, leading to carbohydrate depletion and eventual die-off (Alcoverro et al., 1999; Ralph et al., 2007; Hintz et al., 2022). In agreement, we observed F_v/F_m values falling below 0.2 and near-total biomass collapse under EL conditions, indicating severe photoinhibition and insufficient photochemical energy to support net carbon gain. Such extremely low F_v/F_m values (~0.2) imply a large fraction of nonfunctional PSII reaction centers (Gorbinov and Falkowski, 2022), a pattern commonly observed in seagrasses that are dead or dying (Biber et al., 2004) when light falls below minimum requirements (Bertelli and Unsworth, 2018). For context, unstressed leaves typically show $F_v/F_m \approx 0.83$ (Björkman and Demmig, 1987).

Conversely, NH₄Cl enrichment did not elicit significant stress responses under our high-light conditions, in line with mesocosm evidence showing that ammonium becomes deleterious primarily when combined with low light, whereas no such effects occur under high light; moreover, moderate (<10 μM) DIN can even stimulate growth when nutrient-limited (Villazán et al., 2013). At higher concentrations, ammonium toxicity in *Z. marina* is well documented (Van Katwijk et al., 1997).

Shading shifted plant carbon balance from accrual to expenditure, consistent with reported NSC depletion and declines in both aboveground and belowground biomass (Burke et al., 1996). In our experiment, the increase in aboveground loss and the decline

of belowground mass are consistent with a canopy-thinning strategy that lowers whole-plant respiratory demand, while mobilizing rhizome carbohydrates to sustain metabolism under low light (Wong et al., 2021). This dynamic aligns with seagrass light-stress theory: rapid photophysiological impairment under shading precedes growth and survival losses as net carbon balance turns negative (Ralph et al., 2007; Bertelli and Unsworth, 2018). Consequently, the observed decrease in below-ground carbon content provides a strong signature of carbon limitation.

Antioxidant enzyme responses were variable among treatments. In our study, POD activity increased under reduced irradiance, while SOD, CAT and GSH-Px showed no consistent trends, which is plausible under diminished photo-oxidative pressure (lower excitation energy at PSII/PSI) where ROS generation is limited by reductant availability (Foyer and Noctor, 2016). Such responses are consistent with the view that oxidative stress in seagrasses is context-dependent—shaped by light history, stress duration and co-stressors (Bertelli and Unsworth, 2018; Costa et al., 2021). Importantly, our MDA results—no increase under shading and occasionally higher values under high irradiance—support a mechanism where low light does not exacerbate oxidative damage, but higher ROS generation occurs when photosynthetic electron transport is more active, in line with chloroplast “push-pull” redox theory (Foyer and Noctor, 2016), and with observations that increases in light or temperature do not necessarily elevate MDA levels in seagrasses (Costa et al., 2021).

Across traits, NH₄Cl enrichment alone showed minimal main effects, consistent with evidence that low–moderate inorganic N

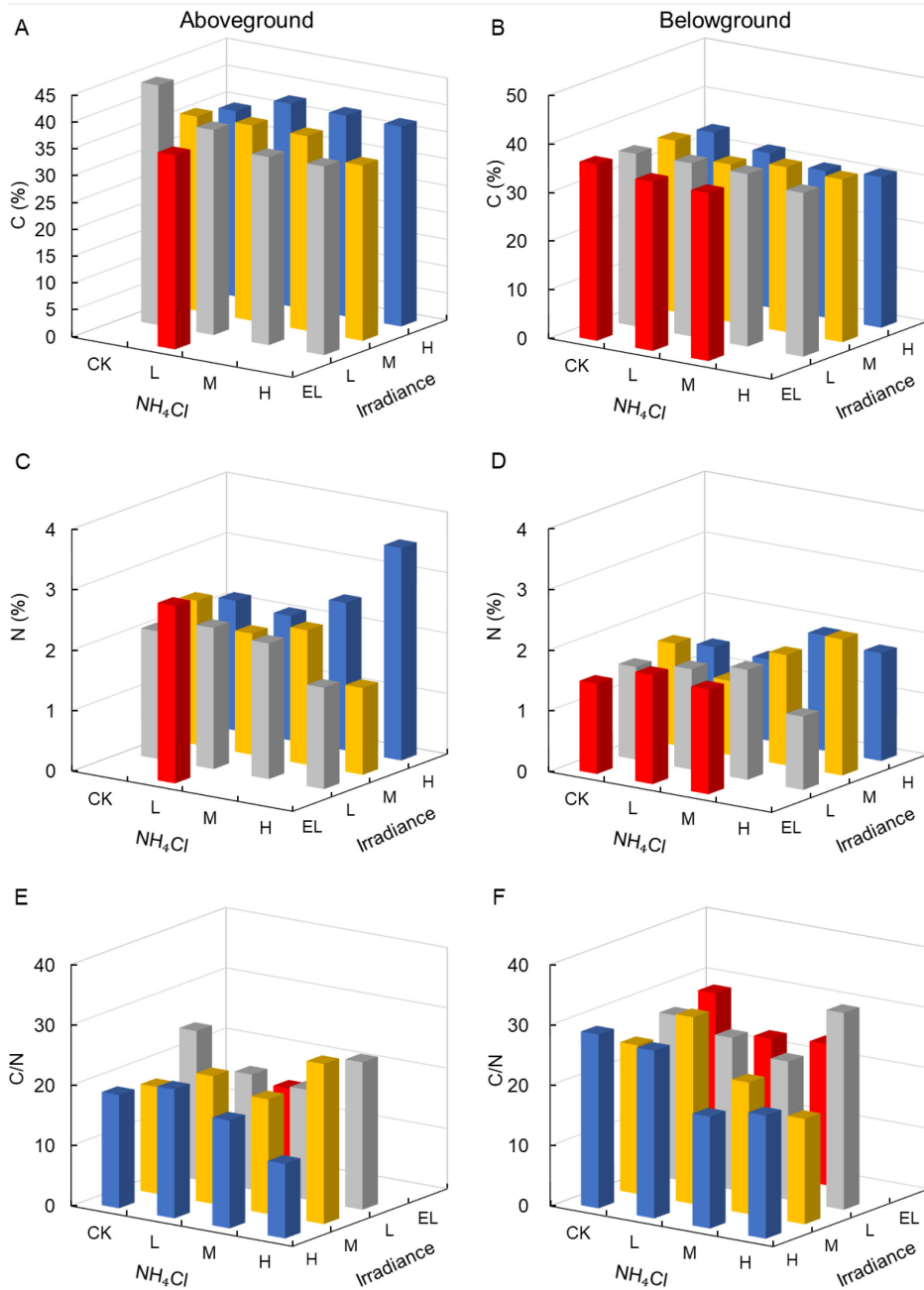


FIGURE 6 Carbon and nitrogen content and C:N ratios in *Zostera marina* under gradients of light intensity and NH_4Cl enrichment. (A) Aboveground carbon content; (B) Belowground carbon content; (C) Aboveground nitrogen content; (D) Belowground nitrogen content; (E) Aboveground C:N ratio; (F) Belowground C:N ratio. Irradiance levels (H, M, L, EL) and NH_4Cl addition levels (CK, L, M, H) are indicated consistently across figures using the same color scheme and axis orientation, as defined in Section 2.1.

additions, typically reported at concentrations $<10 \mu\text{M}$ may stimulate seagrass growth rather than cause toxicity (Touchette and Burkholder, 2000; Villazán et al., 2013). Ammonium toxicity in *Z. marina* typically emerges at relatively high water-column concentrations—on the order of $\sim 10^2 \mu\text{M}$ —and can be exacerbated by low light (Van Katwijk et al., 1997). Because our highest addition ($100 \mu\text{mol L}^{-1}$) sits close to this lower toxicity bound, we interpret the weak ammonium responses as conditional on the short experimental duration and light context, and anticipate that clearer effects could develop with longer exposure and/or under stronger light limitation. Given that light limitation is a primary

proximal stressor for seagrasses, and eutrophication often depresses performance via indirect light reduction (Ralph et al., 2007), our data align with the view that N effects are contingent on concentration and context, whereas light is the dominant immediate driver in this experiment.

Isotopically, both aboveground and belowground $\delta^{15}\text{N}$ declined with NH_4Cl addition, consistent with assimilation of ^{15}N -depleted ammonium and isotope fractionation during uptake/assimilation (Ariz et al., 2011; Foscari et al., 2021). Leaf $\delta^{15}\text{N}$ is widely used to trace nitrogen sources in seagrass and coastal producers, with lower values indicating greater reliance on ammonium when source $\delta^{15}\text{N}$

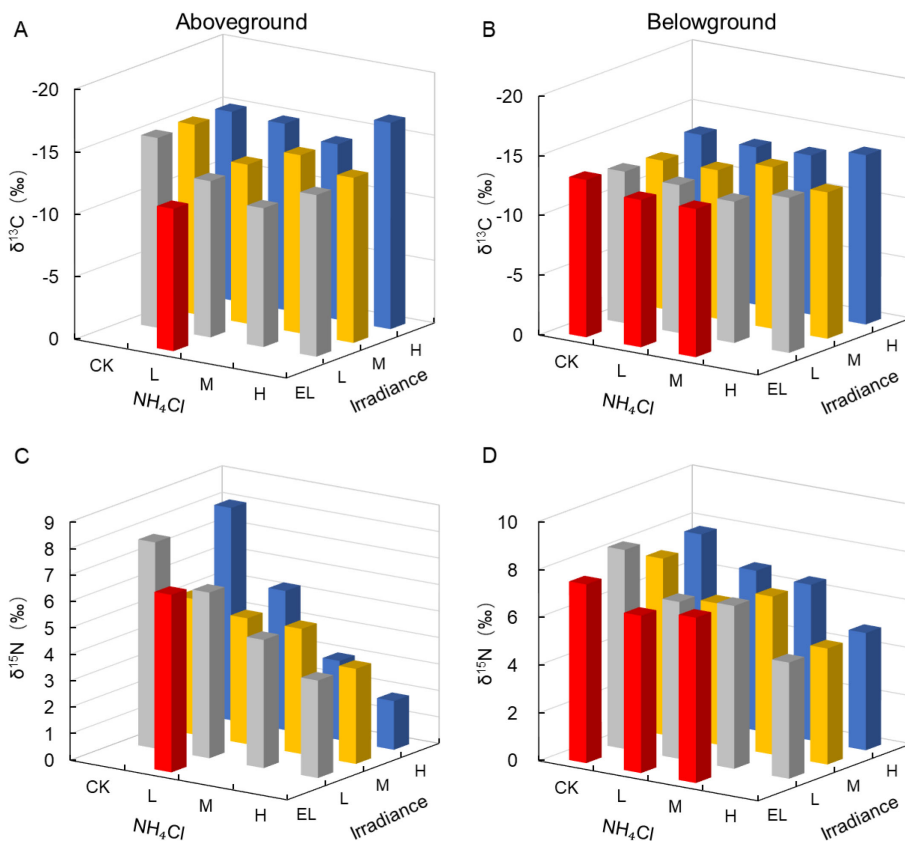


FIGURE 7
 Stable isotope composition ($\delta^{13}\text{C}$ and $\delta^{15}\text{N}$) in *Zostera marina* under gradients of light intensity and NH_4Cl enrichment. (A) Aboveground $\delta^{13}\text{C}$; (B) Belowground $\delta^{13}\text{C}$; (C) Aboveground $\delta^{15}\text{N}$; (D) Belowground $\delta^{15}\text{N}$. Irradiance levels (H, M, L, EL) and NH_4Cl addition levels (CK, L, M, H) are indicated consistently across figures using the same color scheme and axis orientation, as defined in Section 2.1.

and/or uptake fractionation favor ^{14}N (Kahmen et al., 2008; Jones et al., 2018). In *Z. marina*, DIN-uptake/ $\delta^{15}\text{N}$ studies support this interpretation, so the observed $\delta^{15}\text{N}$ shift provides an internal tracer corroborating NH_4^+ assimilation despite minimal whole-plant morphological/physiological responses (Robinson, 2001; Sandoval-Gil et al., 2015).

The present experimental design does not explicitly separate direct ammonium uptake through leaves from indirect effects mediated via sediment processes. Ammonium was added to the water column, and given the relatively short experimental duration, direct uptake by aboveground tissues likely contributed substantially to the observed nitrogen-related responses. This interpretation is supported by previous uptake studies showing that maximum ammonium uptake rates in aboveground tissues of *Z. marina* are substantially higher than those in belowground tissues (approximately 2.6-fold) (Li et al., 2020). Nevertheless, sediment-mediated processes, including microbial transformation and changes in sediment nitrogen availability, may also contribute to plant nitrogen acquisition, particularly over longer timescales (Herbert, 1999).

Although treatment effects on $\delta^{13}\text{C}$ were not statistically significant, we observed a slight tendency toward less negative values under EL–L (–11.4‰) relative to H (–14 to –16.5‰). We note, however, that most experimental and review studies report $\delta^{13}\text{C}$ enrichment under higher irradiance, as increased

photosynthetic demand and boundary-layer drawdown (and/or greater HCO_3^- use) reduce discrimination, yielding less negative $\delta^{13}\text{C}$ (Grice et al., 1996; Hemminga and Mateo, 1996; Lepoint et al., 2004). Conversely, shading typically increases discrimination and drives more negative $\delta^{13}\text{C}$ (Durako and Hall, 1992). Our non-significant pattern should therefore be interpreted cautiously and may reflect transient DIC speciation, site-specific boundary-layer conditions, or tissue turnover effects. One possible explanation is that leaf and rhizome $\delta^{13}\text{C}$ reflect carbon acquisition integrated over tissue turnover times that may exceed the five-week experimental duration, thereby constraining the development of strong isotopic responses under short-term light manipulation.

We acknowledge that this unreplicated factorial design limits formal statistical inference and precludes testing for interaction effects. Consequently, the present results should be interpreted as indicative of dominant main effects during early response stages, rather than as definitive tests of light \times nitrogen interactions under the present experimental design.

5 Conclusion

Our controlled microcosm shows that irradiance, not ammonium enrichment within 0–100 $\mu\text{mol L}^{-1}$, governs the early

trajectory of *Zostera marina*. Shading depressed shoot density, AGB, BGB and F_v/F_m , increased tissue turnover, and reduced below-ground carbon—an integrated signature of light-driven carbon limitation. In contrast, NH_4Cl produced minimal main effects on morphology, pigments, F_v/F_m or MDA and yielded isotopic, not structural, evidence of uptake via declining $\delta^{15}\text{N}$. Antioxidant responses were variable (POD increase; other enzymes inconsistent), and MDA did not rise under shading, consistent with reduced excitation pressure at low light. Collectively, these results argue for tiered diagnostics: rapid photophysiology (F_v/F_m) to flag approaching thresholds, structural metrics (shoot density, AGB/BGB, turnover) to quantify functional loss, and integrative biogeochemical markers (below-ground C; δ -isotopes) to assess resource balance. From a management perspective, maintaining water clarity to meet species-specific minimum light requirements remains paramount, which can be operationalized in practice using routinely available optical proxies such as underwater PAR, Secchi depth, or turbidity-based estimates within existing coastal monitoring programs; nitrogen effects are context- and dose-dependent. Methodologically, the absence of within-cell replication precluded formal interaction tests, so subtle light \times NH_4^+ effects may have been missed. Longer exposures and graded NH_4^+ treatments should explicitly resolve interaction thresholds and link optical conditions to % surface-light targets, while direct NSC measurements will strengthen inferences connecting photophysiology, turnover and survival.

Data availability statement

The raw data supporting the conclusions of this article will be made available by the authors, without undue reservation.

Author contributions

SX: Investigation, Writing – review & editing, Software, Funding acquisition, Data curation, Writing – original draft, Visualization. GY: Writing – original draft, Investigation. XW: Writing – original draft, Investigation. YY: Writing – original draft, Investigation. YW: Writing – original draft, Investigation. ML: Writing – original draft, Investigation. YuZ: Writing – original draft, Investigation. SY: Investigation, Writing – original draft. XZ:

Investigation, Writing – original draft. YiZ: Writing – review & editing.

Funding

The author(s) declared that financial support was received for this work and/or its publication. This research was supported by the Young Scientists Fund of the National Natural Science Foundation of China (42206142), Shandong Provincial Natural Science Foundation (ZR2024QD102), and the Taishan Scholars Program (Distinguished Taishan Scholars).

Conflict of interest

The author(s) declared that this work was conducted in the absence of any commercial or financial relationships that could be construed as a potential conflict of interest.

Generative AI statement

The author(s) declared that generative AI was not used in the creation of this manuscript.

Any alternative text (alt text) provided alongside figures in this article has been generated by Frontiers with the support of artificial intelligence and reasonable efforts have been made to ensure accuracy, including review by the authors wherever possible. If you identify any issues, please contact us.

Publisher's note

All claims expressed in this article are solely those of the authors and do not necessarily represent those of their affiliated organizations, or those of the publisher, the editors and the reviewers. Any product that may be evaluated in this article, or claim that may be made by its manufacturer, is not guaranteed or endorsed by the publisher.

References

- Alcoverro, T., Zimmerman, R. C., Kohrs, D. G., and Alberte, R. S. (1999). Resource allocation and sucrose mobilization in light-limited eelgrass *Zostera marina*. *Mar. Ecol. Prog. Ser.* 187, 121–131. doi: 10.3354/meps187121
- Ariz, I., Cruz, C., Moran, J. F., González-Moro, M. B., García-Olaverri, C., González-Murua, C., et al. (2011). Depletion of the heaviest stable N isotope is associated with $\text{NH}_4^+/\text{NH}_3$ toxicity in NH_4^+ -fed plants. *BMC Plant Biol.* 11, 83. doi: 10.1186/1471-2229-11-83
- Ballesteros, E., Cebrian, E., and Alcoverro, T. (2007). Mortality of shoots of *Posidonia oceanica* following meadow invasion by the red alga *Lophocladia lallemandii*. *Botanica Mar.* 50(1), 8–13. doi: 10.1515/BOT.2007.002
- Bertelli, C. M., and Unsworth, R. K. F. (2018). Light stress responses by the eelgrass, *Zostera marina* (L.). *Front. Environ. Sci.* 6, 00039. doi: 10.3389/fenvs.2018.00039
- Biber, P. D., Paerl, H. W., Gallegos, C. L., and Kenworthy, W. J. (2004). *Evaluating indicators of seagrass stress to light. Estuarine indicators* (Boca Raton, FL, USA: CRC Press), 215–232.
- Björkman, O., and Demmig, B. (1987). Photon yield of O_2 evolution and chlorophyll fluorescence characteristics at 77 K among vascular plants of diverse origins. *Planta* 170, 489–504. doi: 10.1007/BF00402983
- Bulmer, R. H., Townsend, M., Drylie, T., and Lohrer, A. M. (2018). Elevated turbidity and the nutrient removal capacity of seagrass. *Front. Mar. Sci.* 5, 462. doi: 10.3389/fmars.2018.00462

- Burke, M. K., Dennison, W. C., and Moore, K. A. (1996). Non-structural carbohydrate reserves of eelgrass *Zostera marina*. *Mar. Ecol. Prog. Ser.* 137, 195–201. doi: 10.3354/meps137195
- Collier, C. J., Chartrand, K., Honchin, C., Fletcher, A., and Rasheed, M. (2016). Light thresholds for seagrasses of the GBRWHA: a synthesis and guiding document. *Report*. James Cook University, Cairns, Australia.
- Collos, Y., and Harrison, P. J. (2014). Acclimation and toxicity of high ammonium concentrations to unicellular algae. *Mar. pollut. Bull.* 80, 8–23. doi: 10.1016/j.marpolbul.2014.01.006
- Costa, M. M., Silva, J., Barrote, I., and Santos, R. (2021). Heatwave effects on the photosynthesis and antioxidant activity of the seagrass *Cymodocea nodosa* under contrasting light regimes. *Ocean 2* (3), 448–460. doi: 10.3390/oceans2030025
- Dazy, M., Masfaraud, J.-F., and Féraud, J.-F. (2009). Induction of oxidative stress biomarkers associated with heavy metal stress in *Fontinalis antipyretica* Hedw. *Chemosphere* 75, 297–302. doi: 10.1016/j.chemosphere.2008.12.045
- Dennison, W. C., Orth, R. J., Moore, K. A., Stevenson, J. C., Carter, V., Kollar, S., et al. (1993). Assessing water quality with submersed aquatic vegetation. *BioScience* 43, 86–94. doi: 10.2307/1311969
- Duarte, C. M. (1991). Seagrass depth limits. *Aquat. Bot.* 40, 363–377. doi: 10.1016/0304-3770(91)90081-F
- Duarte, C. M., Middelburg, J. J., and Caraco, N. (2005). Major role of marine vegetation on the oceanic carbon cycle. *Biogeosciences* 2, 1–8. doi: 10.5194/bg-2-1-2005
- Durako, M. J., and Hall, M. O. (1992). Effects of light on the stable carbon isotope composition of the seagrass *Thalassia testudinum*. *Mar. Ecol. Prog. Ser.* 86, 99–101. doi: 10.3354/meps086099
- Foscari, A., Leonarduzzi, G., and Incerti, G. (2021). N uptake, assimilation and isotopic fractioning control $\delta^{15}\text{N}$ dynamics in plant DNA: A heavy labelling experiment on *Brassica napus* L. *PLoS One* 16, e0247842. doi: 10.1371/journal.pone.0247842
- Foyer, C. H., and Noctor, G. (2016). Stress-triggered redox signalling: what's in pROSpect? *Plant. Cell Environ.* 39, 951–964. doi: 10.1111/pce.12621
- Gorbunov, M. Y., and Falkowski, P. G. (2022). Using chlorophyll fluorescence to determine the fate of photons absorbed by phytoplankton in the World's oceans. *Annu. Rev. Mar. Sci.* 14, 213–238. doi: 10.1146/annurev-marine-032621-122346
- Green, E. P., and Short, F. T. (2003). *World atlas of seagrasses* (Berkeley, CA, USA: University of California Press).
- Grice, A., Loneragan, N., and Dennison, W. (1996). Light intensity and the interactions between physiology, morphology and stable isotope ratios in five species of seagrass. *J. Exp. Mar. Biol. Ecol.* 195, 91–110. doi: 10.1016/0022-0981(95)00096-8
- Hemminga, M., and Mateo, M. (1996). Stable carbon isotopes in seagrasses: variability in ratios and use in ecological studies. *Mar. Ecol. Prog. Ser.* 140, 285–298. doi: 10.3354/meps140285
- Herbert, R. (1999). Nitrogen cycling in coastal marine ecosystems. *FEMS Microbiol. Rev.* 23, 563–590. doi: 10.1111/j.1574-6976.1999.tb00414.x
- Hintz, N. H., Schulze, B., Wacker, A., and Striebel, M. (2022). Ecological impacts of photosynthetic light harvesting in changing aquatic environments: A systematic literature map. *Ecol. Evol.* 12, e8753. doi: 10.1002/ece3.8753
- Hodges, D. M., DeLong, J. M., Forney, C. F., and Prange, R. K. (1999). Improving the thiobarbituric acid-reactive-substances assay for estimating lipid peroxidation in plant tissues containing anthocyanin and other interfering compounds. *Planta* 207, 604–611. doi: 10.1007/s004250050524
- Jones, B. L., Cullen-Unsworth, L. C., and Unsworth, R. K. (2018). Tracking nitrogen source using $\delta^{15}\text{N}$ reveals human and agricultural drivers of seagrass degradation across the British Isles. *Front. Plant Sci.* 9, 133. doi: 10.3389/fpls.2018.00133
- Kahmen, A., Wanek, W., and Buchmann, N. (2008). Foliar $\delta^{15}\text{N}$ values characterize soil N cycling and reflect nitrate or ammonium preference of plants along a temperate grassland gradient. *Oecologia* 156, 861–870. doi: 10.1007/s00442-008-1028-8
- Kent, F., Lilley, R., Unsworth, R., Cunningham, S., Begg, T., Boulcott, P., et al. (2021). Seagrass restoration in Scotland—handbook and guidance. *NatureScot Research Report* 1286.
- Lee, K. S., Park, S. R., and Kim, Y. K. (2007). Effects of irradiance, temperature, and nutrients on growth dynamics of seagrasses: A review. *J. Exp. Mar. Biol. Ecol.* 350, 144–175. doi: 10.1016/j.jembe.2007.06.016
- Lepoint, G., Dauby, P., and Gobert, S. (2004). Applications of C and N stable isotopes to ecological and environmental studies in seagrass ecosystems. *Mar. pollut. Bull.* 49, 887–891. doi: 10.1016/j.marpolbul.2004.07.005
- Li, S.-Q., Zhang, Y.-H., Li, Z., and Zhang, P.-D. (2020). Uptake kinetics of nitrogen and phosphorus by *Zostera marina*. *Chin. J. Plant Ecol.* 44, 772. doi: 10.17521/cjpe.2019.0335
- Lichtenthaler, H. (1987). Chlorophylls and carotenoids: pigments of photosynthetic biomembranes. *Methods Enzymol.* 148, 350–382. doi: 10.1016/0076-6879(87)48036-1
- Makino, A., Mae, T., and Ohira, K. (1985). Enzymic properties of ribulose-1, 5-bisphosphate carboxylase/oxygenase purified from rice leaves. *Plant Physiol.* 79, 57–61. doi: 10.1104/pp.79.1.57
- McMahon, K., Collier, C., and Lavery, P. S. (2013). Identifying robust bioindicators of light stress in seagrasses: A meta-analysis. *Ecol. Indic.* 30, 7–15. doi: 10.1016/j.ecolind.2013.01.030
- Olsen, J. L., Rouzé, P., Verhelst, B., Lin, Y.-C., Bayer, T., Collen, J., et al. (2016). The genome of the seagrass *Zostera marina* reveals angiosperm adaptation to the sea. *Nature* 530, 331–335. doi: 10.1038/nature16548
- Ralph, P. J., Durako, M. J., Enriquez, S., Collier, C. J., and Doblin, M. A. (2007). Impact of light limitation on seagrasses. *J. Exp. Mar. Biol. Ecol.* 350, 176–193. doi: 10.1016/j.jembe.2007.06.017
- Robinson, D. (2001). $\delta^{15}\text{N}$ as an integrator of the nitrogen cycle. *Trends Ecol. Evol.* 16, 153–162. doi: 10.1016/S0169-5347(00)02098-X
- Roca, G., Alcoverro, T., Krause-Jensen, D., Balsby, T. J. S., van Katwijk, M. M., Marbà, N., et al. (2016). Response of seagrass indicators to shifts in environmental stressors: a global review and management synthesis. *Ecol. Indic.* 63, 310–323. doi: 10.1016/j.ecolind.2015.12.007
- Sandoval-Gil, J. M., Camacho-Ibar, V. F., Del Carmen Ávila-López, M., Hernández-López, J., Zertuche-González, J. A., and Cabello-Pasini, A. (2015). Dissolved inorganic nitrogen uptake kinetics and $\delta^{15}\text{N}$ of *Zostera marina* L. (eelgrass) in a coastal lagoon with oyster aquaculture and upwelling influence. *J. Exp. Mar. Biol. Ecol.* 472, 1–13. doi: 10.1016/j.jembe.2015.06.018
- Serrano, O., Gómez-López, D. I., Sánchez-Valencia, L., Acosta-Chaparro, A., Navas-Camacho, R., González-Corredor, J., et al. (2021). Seagrass blue carbon stocks and sequestration rates in the Colombian Caribbean. *Sci. Rep.* 11, 11067. doi: 10.1038/s41598-021-90544-5
- Statton, J., McMahon, K., McCallum, R., Armstrong, P., Dunham, N., Strydom, S., et al. (2017). Determining light stress bio-indicators and thresholds for a tropical multi-species seagrass assemblage. Report of Theme 5 - Project 5.5.1 prepared for the Dredging Science Node, Western Australian Marine Science Institution, Perth, Western Australia, 50 pp.
- Touchette, B. W., and Burkholder, J. M. (2000). Review of nitrogen and phosphorus metabolism in seagrasses. *J. Exp. Mar. Biol. Ecol.* 250, 133–167. doi: 10.1016/S0022-0981(00)00195-7
- Unsworth, R. K. F., Nordlund, L. M., and Cullen-Unsworth, L. C. (2018). Seagrass meadows support global fisheries production. *Conserv. Lett.* 12 (1), e12566. doi: 10.1111/conl.12566
- Van Katwijk, M. M., Van Beusekom, J. E., Folmer, E. O., Kolbe, K., De Jong, D. J., and Dolch, T. (2024). Seagrass recovery trajectories and recovery potential in relation to nutrient reduction. *J. Appl. Ecol.* 61, 1784–1804. doi: 10.1111/1365-2664.14704
- Van Katwijk, M., Vergeer, L., Schmitz, G., and Roelofs, J. (1997). Ammonium toxicity in eelgrass *Zostera marina*. *Mar. Ecol. Prog. Ser.* 157, 159–173. doi: 10.3354/meps157159
- Villazán, B., Pedersen, M. F., Brun, F. G., and Vergara, J. J. (2013). Elevated ammonium concentrations and low light form a dangerous synergy for eelgrass *Zostera marina*. *Mar. Ecol. Prog. Ser.* 493, 141–154. doi: 10.3354/meps10517
- Wong, M. C., Vercaemer, B. M., and Griffiths, G. (2021). Response and recovery of eelgrass (*Zostera marina*) to chronic and episodic light disturbance. *Estuar. Coasts.* 44, 312–324. doi: 10.1007/s12237-020-00803-3
- Zhang, Y., Yue, S., Gao, Y., Zhao, P., Liu, M., Qiao, Y., et al. (2024). Insights into response of seagrass (*Zostera marina*) to sulfide exposure at morphological, physiochemical and molecular levels in context of coastal eutrophication and warming. *Plant. Cell Environ.* 47, 4768–4785. doi: 10.1111/pce.15048